

Li on bond-center sites in Si

U. Wahl,* M. Restle, C. Ronning, and H. Hofsäss
Fakultät für Physik, Universität Konstanz, D-78434 Konstanz, Germany

S. G. Jahn
ISOLDE Collaboration, CERN, CH-1211 Geneva 23, Switzerland
 (Received 27 January 1994)

Radioactive Li ions were implanted into high-resistivity *p*-type Si at temperatures between 40 and 530 K and their lattice sites determined by measuring the channeling and blocking effects of the emitted alpha particles. Implantations below room temperature lead to the occupation of the well-known tetrahedral interstitial sites, whereas for implantations above room temperature bond-center sites could be unambiguously identified. As cause of the corresponding lattice site changes, an interaction of diffusing Li with double vacancies is suggested.

I. INTRODUCTION

The alkali-metal Li has unusual properties when incorporated in silicon; in its isolated form, it acts as one of the shallowest donors known,¹ therefore, being mostly positively charged. It also belongs, together with hydrogen and copper, to the fastest diffusing foreign atoms,² due to its preference for interstitial lattice sites. The combination of both properties results in the strong interaction of Li with additional defects, due to its positive charge preferentially with negative defects, but also with neutral defects like oxygen. From the viewpoint of basic semiconductor research, this makes Li atoms interesting probes which, in some respects, are comparable to protons, muons, or positrons and can be used for the investigation of intrinsic defects or impurities in semiconductors. The interaction of additional defects with Li may influence specific properties of the Li atoms remarkably, e.g., their lattice site or diffusion constant and, therefore, the study of these properties may also yield information on the presence of those defects. On the other hand, Li is not suitable as a thermally stable dopant for the same reasons, and the main technological applications of Li in semiconductors all rely on its interaction with other defects. The most prominent examples are Li-compensated particle detectors [Si(Li), Ge(Li)], which have been used with great success in nuclear radiation spectroscopy.³ The passivating effect of Li on acceptor-type defects is used to construct *p-i-n* diodes from Si or Ge single crystals with both extremely high resistivity and good charge-carrier mobility in the intrinsic layer. In the case of Si(Li) detectors for particle and x-ray spectroscopy in the keV range, the quality of these solid-state detectors has not been achieved by other means as yet.

It is interesting to compare Li to hydrogen and muonium. These species may occupy both near-tetrahedral and bond-centered interstitial sites in Si, depending on their charge states and interactions with other defects.^{4,5} In the case of Li in high-purity Si, the only lattice site clearly identified so far is the tetrahedral site.^{1,6} It is known that Li may passivate the electrical activity of vacancy-

like defects in Si.⁷ Photoluminescence studies revealed the existence of a defect complex consisting of four Li atoms and, presumably, a single or double vacancy.⁸ This complex exhibited trigonal symmetry, indicating that one Li atom occupied a unique site in the complex. Theoretical studies were able to explain, e.g., the passivation of the single vacancy by the formation of $(\text{Li}_4^+ \text{V}^{4-})^0$ complexes with Li occupying neighboring interstitial sites.⁹ After irradiation of Li-doped Si with 5-MeV neutrons, an interaction of Li with divacancies was observed by infrared (IR) absorption spectroscopy and attributed to the formation of (LiV_2) complexes.¹⁰ However, very little experimental knowledge on the microscopic structure and accordingly on the lattice sites of Li in any such complexes is available. In this paper we will give direct evidence for Li atoms occupying bond-center sites after ion implantation into high-resistivity *p*-type Si.

The emission-channeling technique, which was discovered in 1965 (Ref. 11) and has recently been reviewed,¹² is a sensitive method for lattice location of foreign atoms in single crystals. Charged particles, which are emitted from radioactive atoms, experience channeling or blocking effects along crystal axes and planes. By detecting the angular-dependent emission yield of particles outside the crystal with respect to major crystal directions, the lattice sites of the emitting atoms may be determined. Using the isotope ^8Li ($t_{1/2} = 838$ ms), which decays into an excited state of ^8Be that immediately breaks up into two α particles with energies continuously distributed around 1.6 MeV,¹³ Lindner *et al.* were able to show lattice site changes of Li from tetrahedral to substitutional sites in GaAs.¹⁴ Since these experiments, we have improved the sensitivity of the ^8Li α -emission-channeling technique considerably by introducing position-sensitive detection methods¹⁵ and, recently, by combining it with large-scale Monte Carlo calculations of the corresponding two-dimensional emission patterns.

II. EXPERIMENT

^8Li was produced at the on-line isotope separator PSB-ISOLDE at CERN (Ref. 16) by nuclear reactions of

a 1-GeV proton beam with a heated Ta target, and, after ionization and mass separation, was available as an isotopically pure 60-keV ion beam. ^8Li implantations with a collimated beam (0.5 mm diameter) into single crystals of Si at varying temperature were performed with the setup described previously.¹² For detecting the angular dependence of emitted α particles in a range of $\pm 2^\circ$, we used a two-dimensional position-sensitive Si detector.¹⁷ The total angular resolution of the measurements due to the size of the beam spot and the detector resolution was $\sigma = 0.12^\circ$. The depth profile after 60-keV implantation of ^8Li into Si can be approximated using the computer simulation program TRIM (Ref. 18) as near Gaussian with $\sigma = 620 \text{ \AA}$ and centered at $x_0 = 3620 \text{ \AA}$. The implantation doses were as low as $1 \times 10^{12} \text{ cm}^{-2}$ per channeling pattern and did not accumulate to more than $2 \times 10^{13} \text{ cm}^{-2}$ on a single beam spot. This is far below the dose needed for amorphization of Si by implantation of light ions, e.g., for the heavier ion ^{11}B this dose is about 10^{15} cm^{-2} at 100 K and above 10^{16} cm^{-2} at room temperature.¹⁹ The *p*-type Si samples were a $\langle 111 \rangle$ -oriented single crystal of 10 k Ω cm (electrically active acceptor concentration about $1.5 \times 10^{12} \text{ cm}^{-3}$, probably boron) and a $\langle 100 \rangle$ -oriented crystal of 100 Ω cm (B-doped, $[\text{B}] = 1.3 \times 10^{14} \text{ cm}^{-3}$). Both were cut from float-zone (FZ) purified wafers from Wacker Chemitronics. Calculations of channeling and blocking effects were done using the Monte Carlo simulation program FLUX developed by Smulders and Boerma.²⁰ Details of the parameters used in the simulations are described elsewhere.²¹

III. RESULTS

As was theoretically derived by Lindhard²² and experimentally confirmed, e.g., by Andersen and Uggerhoj,²³ emission-channeling patterns can be interpreted in the same way as results obtained from foreign-atom-location studies with an external analyzing ion beam. For example, if in a Rutherford backscattering (RBS) experiment the lattice site of foreign atoms would be extracted from the backscattered yield of α particles as a function of their incidence angle with the crystal axes $\langle 111 \rangle$, $\langle 100 \rangle$, and $\langle 110 \rangle$, we can obtain the same information with radioactive probe atoms from the α -emission yield around those axes. This holds as long as irreversible processes like electronic energy loss are negligible and if proper correspondence between experimental parameters is made, e.g., beam divergence in the case of RBS corresponds to the angular resolution due to the position resolution of the detector and the size of the beam spot in emission channeling.

Figure 1(a) shows the normalized α -emission yield in the vicinity of the $\langle 110 \rangle$ axis of the 10 k Ω cm single crystal during implantation of ^8Li at 293 K. The channeling effects along the axial $\langle 110 \rangle$ and planar $\{111\}$ and $\{311\}$ directions, in combination with the blocking effects along planar $\{110\}$ and $\{100\}$ directions, give clear evidence that a large fraction of the emitter atoms occupies tetrahedral interstitial sites. This can be seen directly from a comparison of the experimental data to the two-dimensional emission pattern that is obtained as a result

of Monte Carlo calculations assuming 100% of ^8Li atoms on tetrahedral sites [Fig. 1(b)]. In contrast to that, for an implantation temperature of $T_i = 425 \text{ K}$ we obtain weak blocking effects along the $\langle 110 \rangle$ axis and $\{110\}$ and $\{111\}$ planes and channeling effects along the $\{100\}$ and $\{311\}$ planes [Fig. 1(c)]. The changes in the character of the $\langle 110 \rangle$, $\{111\}$, and $\{100\}$ effects clearly indicate site changes of a large fraction of ^8Li away from the tetrahedral positions.

Quantitative information on the fractions of ^8Li emitter atoms on different lattice sites and on their thermal vibrational amplitudes may be obtained by fitting superpositions of theoretical emission patterns to the experimental data.²¹ For this purpose, theoretical patterns were calculated for emitter atoms on tetrahedral, substitutional, bond-center, antibonding, hexagonal, and the so-called *Y* and *C* sites with varying thermal vibrational amplitudes, as well as for displacements between all those sites. For the room-temperature results, a very good correspondence between experimental and theoretical data was obtained for 76(3)% of ^8Li on tetrahedral sites with a mean one-dimensional thermal vibration amplitude of $u_1 = 0.13(2) \text{ \AA}$, and 24(3)% on completely irregular ("random") sites, which are assumed to produce no anisotropies in the emission yield. Introducing fractions on other lattice sites did not significantly improve the quality of the fits in this case, though the random fraction may include small contributions from low-symmetry lattice sites, e.g., the detection limit for occupation of bond-center sites was found around 15%. For the implantation temperature of $T_i = 425 \text{ K}$, however, the agreement was best for 54(10)% of ^8Li on bond-center (BC) sites, 10(2)% on tetrahedral (*T*) sites, and 36(10)% on random (*R*) sites [Fig. 1(d)]. Static or dynamic displacements from these sites must, in this case, be less than 0.4 \AA in order to be compatible with the experimental results. For larger displacements, the quality of the fits deteriorated markedly, while the corresponding site fractions were not too sensitive ($\pm 2\%$ for *T*, $\pm 10\%$ for BC) on displacements within the given limits. As a consequence, the thermal vibrational amplitudes of ^8Li for both *T* and BC sites were treated as fixed parameters in these fits and calculated from an effective Debye temperature²⁴ of ^8Li , which is estimated from the Debye temperature of Si by $T_D(^8\text{Li}) = (28/8)^{1/2} T_D(^{28}\text{Si})$. If $T_D(\text{Si}) = 490 \text{ K}$ is used,²⁵ this yields $T_D(^8\text{Li}) = 917 \text{ K}$, and $u_1 = 0.10 \text{ \AA}$ at $T = 425 \text{ K}$.

Calculating the channeling patterns from BC sites, it is important to use the proper emitter depth profile. For shallow profiles ($\lesssim 1000 \text{ \AA}$) channeling effects along $\{111\}$ planes are obtained, deeper lying profiles (as in our case) will cause blocking effects due to pronounced dechanneling along these planes. This effect will be discussed in more details in a forthcoming publication. We strongly suspect that it is also responsible for some of the inconsistencies between the results of different ion-beam channeling studies on the lattice location of hydrogen in Si.⁵ In α -emission-channeling experiments, the measured energy spectrum contains direct information about the energy loss of the emitted particles and hence about the depth distribution of emitter atoms. In our experiment,

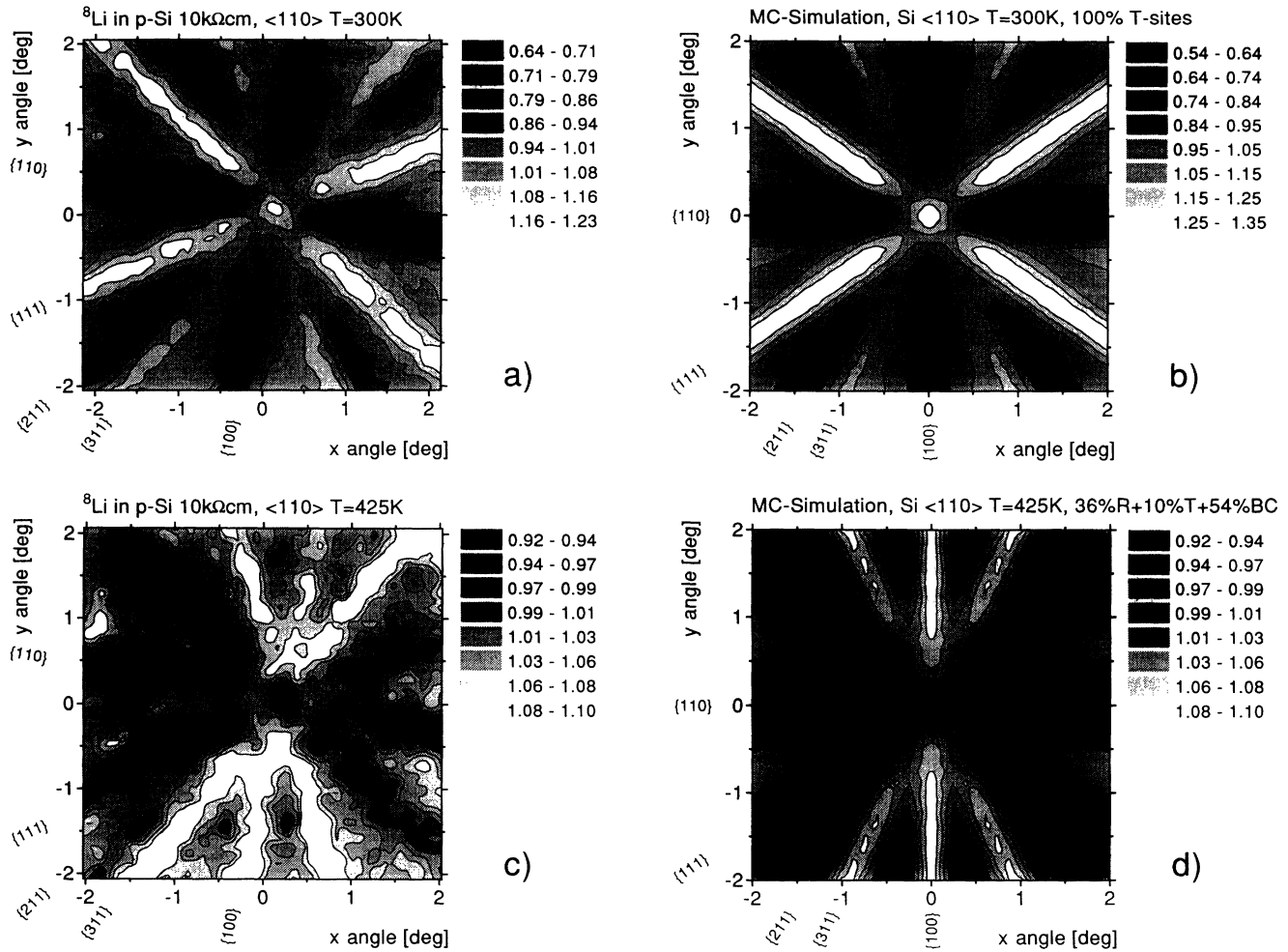


FIG. 1. Normalized α -emission yields from ^8Li in p -type Si in $\pm 2^\circ$ around the $\langle 110 \rangle$ direction: (a) and (c) are experimental patterns, (b) and (d) are simulated patterns for the indicated lattice-site fractions of ^8Li . During the experiment, the Si crystal was mounted in a two-axis goniometer, which does not possess an azimuthal axis of rotation with respect to the detector. The experimental channeling and/or blocking patterns are, therefore, both rotated by 10° with respect to the theoretical patterns.

the shift in the maximum of the $^8\text{Li}/^8\text{Be}^*$ energy distribution between 300 and 525 K was only 10 keV to lower values. In the case of the isotope $^8\text{Li}/\text{Be}^*$, the broad maximum in the α spectrum does not permit a detailed derivation of the Li depth distribution, but using a mean energy loss of 27.5 eV/Å for 1.6-MeV α particles in Si,¹⁸ it is estimated that at the higher temperature the mean value of the ^8Li distribution is only shifted by about 360 Å deeper into the crystal and hence a major redistribution of ^8Li due to long-range diffusion can be excluded in this case.

In an earlier experiment²⁶ ^8Li was implanted between 40 and 530 K into a p -type Si (100 Ω cm) single crystal, and the α -emission yield measured around the $\langle 111 \rangle$, $\langle 100 \rangle$, and $\langle 211 \rangle$ axes. After performing extensive Monte Carlo simulations of the corresponding emission patterns for all different implantation temperatures chosen and applying the same fitting procedures as described above, we are now able to present a quantitative analysis of the occupied ^8Li lattice sites (Fig. 2). As can

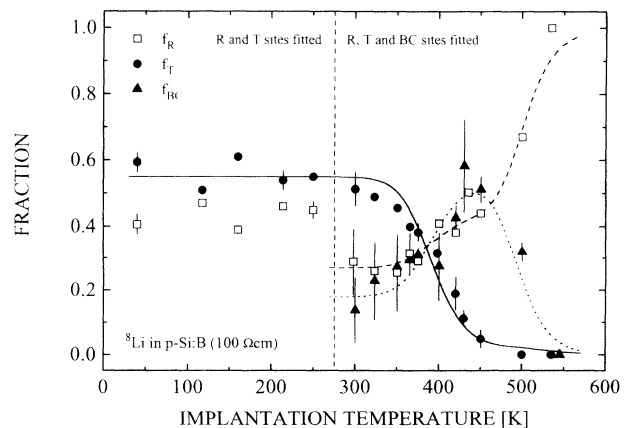


FIG. 2. Lattice site occupancy of ^8Li after implantation into p -type Si (100 Ω cm): T are the tetrahedral sites, BC are the bond-center sites, and R are the random sites.

be seen, the fraction of ^8Li on tetrahedral sites hardly changes between 40 and 300 K. This is by itself an interesting finding as it shows that even after implantation at such low temperatures, 60% of the Li atoms end up on tetrahedral interstitial sites in a rather intact crystalline surrounding. On the contrary, upon increasing the implantation temperature to above 300 K, the amount of Li on BC and random sites rises continuously at the expense of tetrahedral Li. The fraction on BC sites, however, is only stable up to about 500 K, and reaches a maximum of around 50% at 450 K. The *p*-type Si:B (10 k Ω cm) crystal was only investigated above room temperature, where it exhibited a similar behavior, the maximum fraction on BC sites (ca. 60%) being somewhat higher.

IV. DISCUSSION

In the following we will explain why we think that the incorporation of Li on BC sites is related to the capture of diffusing Li by double vacancies. Since the *T* site is the most stable lattice site for isolated Li in Si, the occupancy of BC sites must be due to the interaction with another defect, and either Li or this defect must become mobile above room temperature. Because the mobilization temperature of Si single vacancies is around 100 K for (*V*)⁻ and (*V*)²⁻ and up to around 200 K for (*V*)⁰,²⁷ we conclude that the direct interaction of Li with mobile single vacancies is of no influence for the lattice-site occupancy of ^8Li in high-purity *p*-type Si. This may not be true for very highly *n*-doped Si, where Li was found to occupy substitutional sites.²¹ Previously we have presented²⁶ a simple rate-equation model, which quantitatively describes the capture of $^8\text{Li}^+$ by neutral or negatively charged defects under the assumption that, following the implantation process, ^8Li is initially located on *T* sites, then starts to diffuse and may be captured on its way by a single type of immobile defect. The curves shown in Fig. 2 have been calculated on the basis of a comparable model for two Li-defect complexes, where one is thermally unstable (BC sites) and the other stable (random sites). To account for the random fraction of ^8Li atoms below room temperature, an initial portion of 27% on irregular sites was introduced and regarded as immobile and not available for the formation of other defect complexes. An initial fraction of 18% on BC sites at 300 K was also introduced, much lower fractions on this site may not be distinguished from random sites. The diffusion constant of Li was taken from the literature.² The capture radius of Li^+ at negatively charged defects may be estimated from screened Coulomb potentials to be about 40–50 Å; a capture radius around 5 Å has often been assumed for neutral defects.²⁸ As a compromise we used a fixed value of 20 Å for both *R* and BC sites. Under these assumptions, our experimentally observed site fractions would be well in accordance with a capture of ^8Li by a defect with a concentration of $\approx 2 \times 10^{16} \text{ cm}^{-3}$, leading to the occupation of BC sites in a ^8Li -defect complex. The disappearance of Li on BC sites above 500 K is either due to

annealing of the capturing defect before it is able to trap Li, or to breakup of already formed complexes. In the latter case, if first-order kinetics and an attempt frequency of 10^{13} s^{-1} are assumed, an activation energy of 1.25 eV is estimated for the breakup. Subsequent capture of ^8Li on random sites might be related to a defect in the 10^{16}-cm^3 regime.

Let us now discuss possible candidates: we have to consider both the most abundant impurity atoms and the defects which are created during the implantation of ^8Li . It is reasonable to neglect boron containing defects ($[\text{B}] = 1.3 \times 10^{14}$ and $\approx 1.5 \times 10^{12} \text{ cm}^{-3}$) or clusters of multiple ^8Li atoms (the implantation current of $\approx 6 \times 10^6 \text{ s}^{-1}$ corresponds to a maximum ^8Li concentration of $3 \times 10^{14} \text{ cm}^{-3}$ in the peak of the implantation profile). Some possibility exists for the capture of Li at oxygen-containing defects, e.g., interstitial oxygen or *A* centers (oxygen-vacancy defects), or at carbon. The concentration limits of these elements in the FZ crystals used were $[\text{O}] < 5 \times 10^{15} \text{ cm}^{-3}$ and $[\text{C}] < 10^{16} \text{ cm}^{-3}$. However, the most probable cause for the lattice-site change of ^8Li from *T* to BC sites appears to be due to the implantation-induced defects that contain mainly vacancies. It may easily be estimated, using the simulation program TRIM,¹⁸ that the local concentration of vacancies created close to an implanted ^8Li atom is several orders of magnitudes larger than 10^{16} cm^{-3} . Single vacancies are not stable at 400 K but have recombined or formed secondary defect complexes, which are mainly divacancies in FZ Si.²⁷ The temperature range 430–450 K, where we found the maximum concentration of ^8Li on BC sites, also corresponds rather well to the temperature of 450 K where Chen and Corelli observed a maximum in the IR absorption coefficient of (*LiV*)₂ defects,¹⁰ indicating preferential formation of this defect. These arguments lead us to suggest that ^8Li is captured by double vacancies after implantation into high-purity *p*-type Si at 430 K, occupying the BC site in the center or passivating one of the dangling bonds of the two neighboring vacancies. Watkins and Corbett²⁹ have estimated an activation energy of 1.3 eV for the migration of the divacancy, assuming an attempt frequency of 10^{13} s^{-1} . This value implies that substantial divacancy migration occurs above 500 K and, therefore, above this temperature the population of random sites has to be attributed to Li capture by more extended defects like multiple-vacancy complexes or dislocations.

In summary, we have applied the emission-channeling method in combination with Monte Carlo simulations of complete two-dimensional channeling patterns to identify the lattice sites of ^8Li ion-implanted into high-resistivity *p*-type Si. After implantation below room temperature the well-known tetrahedral interstitial sites were found to be most frequently occupied. Following implantation above room temperature, we have unambiguously identified ^8Li on bond-center sites in Si. We attribute these lattice-site changes to the diffusion of ^8Li and its capture by double vacancies.

- *Present address: Materials Science Center, Rijksuniversiteit Groningen, NL-9747AG Groningen, The Netherlands.
- ¹R. L. Aggarwal, P. Fisher, V. Mourzine, and A. K. Ramdas, *Phys. Rev.* **138**, A882 (1965).
- ²L. T. Canham, *Properties of Silicon* (The Institution of Electrical Engineers, London, 1988).
- ³*Semiconductor Detectors*, edited by G. Bertolini and A. Coche (North-Holland, Amsterdam, 1968).
- ⁴S. M. Myers, M. I. Baskes, H. K. Birnbaum, J. W. Corbett, G. G. DeLeo, S. K. Estreicher, E. E. Haller, P. Jena, N. M. Johnson, R. Kirchheim, S. J. Pearton, and M. J. Stavola, *Rev. Mod. Phys.* **64**, 559 (1992); B. D. Patterson, *ibid.* **60**, 69 (1988).
- ⁵A. D. Marwick, in *Hydrogen in Semiconductors*, edited by J. I. Pankove and N. M. Johnson (Academic, New York, 1991).
- ⁶G. D. Watkins and F. S. Ham, *Phys. Rev. B* **1**, 4071 (1970).
- ⁷G. J. Brucker, *Phys. Rev.* **183**, 712 (1969), and references therein.
- ⁸G. Davies, *Phys. Rep.* **176**, 83 (1989).
- ⁹G. G. DeLeo, W. B. Fowler, and G. D. Watkins, *Phys. Rev. B* **29**, 1819 (1984); E. Tarnow, *J. Phys. Condens. Matter* **4**, 1459 (1992).
- ¹⁰C. S. Chen and J. C. Corelli, *J. Appl. Phys.* **44**, 2483 (1973).
- ¹¹B. Domeij and K. Bjorkqvist, *Phys. Lett.* **14**, 127 (1965).
- ¹²H. Hofsäss and G. Lindner, *Phys. Rep.* **201**, 123 (1991).
- ¹³F. Ajzenberg-Selove, *Nucl. Phys. A* **413**, 1 (1985).
- ¹⁴G. Lindner, S. Winter, H. Hofsäss, S. Jahn, S. Blässer, E. Recknagel, and G. Weyer, *Phys. Rev. Lett.* **63**, 179 (1989).
- ¹⁵U. Wahl, H. Hofsäss, S. G. Jahn, S. Winter, and E. Recknagel, *Nucl. Instrum. Methods. B* **64**, 221 (1992).
- ¹⁶E. Kugler, D. Fiander, B. Jonson, H. Haas, A. Przewloka, H. L. Ravn, D. J. Simon, K. Zimmer, and the ISOLDE collaboration, *Nucl. Instrum. Methods B* **70**, 41 (1992).
- ¹⁷M. Lindroos and Ö. Skeppstedt, *Nucl. Instrum. Methods A* **306**, 225 (1991).
- ¹⁸J. F. Ziegler, J. P. Biersack, and U. Littmark, *The Stopping and Range of Ions in Solids* (Pergamon, New York, 1985).
- ¹⁹J. W. Mayer, L. Eriksson, and J. A. Davies, *Ion Implantation in Semiconductors* (Academic, New York, 1970).
- ²⁰P. J. M. Smulders and D. O. Boerma, *Nucl. Instrum. Methods B* **29**, 471 (1987).
- ²¹U. Wahl, H. Hofsäss, S. G. Jahn, S. Winter, and E. Recknagel, *Appl. Phys. Lett.* **62**, 687 (1993).
- ²²J. Lindhard, *K. Dan. Vidensk. Selsk. Mat. Fys. Medd.* **34** (14) (1965).
- ²³J. U. Andersen and E. Uggerhoj, *Can. J. Phys.* **46**, 517 (1968).
- ²⁴P. G. Dawber and R. J. Elliott, *Proc. R. Soc. London Ser. A* **273**, 222 (1963).
- ²⁵A. Dygo, P. J. M. Smulders, and D. O. Boerma, *Nucl. Instrum. Methods B* **64**, 701 (1992).
- ²⁶U. Wahl, H. Hofsäss, S. G. Jahn, S. Winter, H. Hoffmann, and E. Recknagel, *Nucl. Instrum. Methods B* **63**, 91 (1992).
- ²⁷G. D. Watkins, in *Deep Centers in Semiconductors*, edited by S. T. Pantelides (Gordon and Breach, New York, 1986).
- ²⁸E. M. Pell and F. S. Ham, *J. Appl. Phys.* **32**, 1052 (1961).
- ²⁹G. D. Watkins and J. W. Corbett, *Phys. Rev.* **138**, A543 (1965).

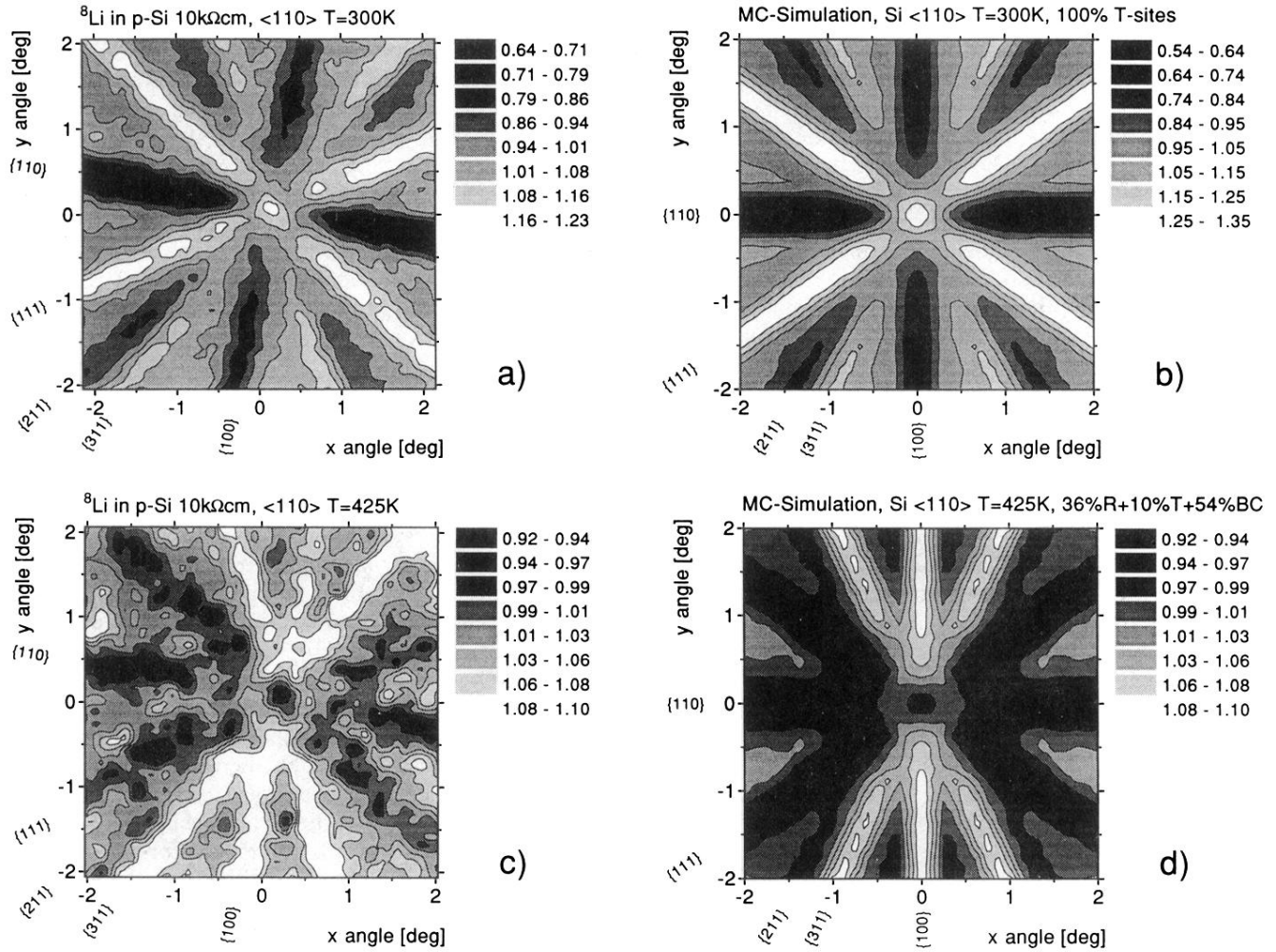


FIG. 1. Normalized α -emission yields from ^8Li in p -type Si in $\pm 2^\circ$ around the $\langle 110 \rangle$ direction: (a) and (c) are experimental patterns, (b) and (d) are simulated patterns for the indicated lattice-site fractions of ^8Li . During the experiment, the Si crystal was mounted in a two-axes goniometer, which does not possess an azimuthal axis of rotation with respect to the detector. The experimental channeling and/or blocking patterns are, therefore, both rotated by 10° with respect to the theoretical patterns.